Desalination 605 (2025) 118706

Contents lists available at ScienceDirect

Desalination

journal homepage: www.elsevier.com/locate/desal

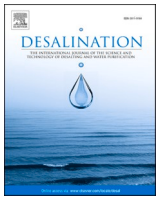

Salinity gradient energy of 109 first-class water systems in Japan

Kotomi Watanabe [a], Yuri Akiba [b], Hiroshi Ishidaira [c], Hiroyuki Shima [a,*]

[a] Department of Environmental Sciences, University of Yamanashi, 4-4-37, Takeda, Kofu, Yamanashi 400-8510, Japan
[b] Mount Fuji Research Institute, Yamanashi Prefectural Government, 5597-1, Kenmarubi, Kamiyoshida, Fujiyoshida, Yamanashi 403-0005, Japan
[c] Interdisciplinary Center for River Basin Environment, University of Yamanashi, 4-3-7, Takeda, Kofu, Yamanashi 400-8511, Japan

HIGHLIGHTS

- Estimated the salinity gradient power (SGP) available at 109 estuaries in Japan
- Compared the SGP values to existing renewable energy output
- Demonstrated theoretically the usefulness of SGP generation in Japan

ABSTRACT

Salinity gradient energy (SGE) is the physico-chemical energy released from an aqueous solution when freshwater is mixed with salt water. SGE is expected to be an alternative energy source that is not affected by weather or time of day, especially near estuaries, where large amounts of water can be taken from rivers and the sea. In this study, we theoretically evaluated the SGE potential and electric power available in 109 major rivers in Japan to identify suitable locations for SGE applications. Furthermore, we examined the usefulness of SGE by comparing the amount of electric power extractable from SGE to that obtained from other power generation methods.

1. Introduction

Securing a source of sustainable and affordable energy is currently one of the most pressing issues facing human society. Since the Industrial Revolution, humans have relied on fossil fuels as a primary energy source for supporting global economic growth. However, once we realized that fossil fuels would become depleted in the future and that their mass consumption would have a major negative impact on the environment, we began searching for new energy sources. Several renewable energy sources have been identified [1–3], among which solar and wind energy have attracted attention because they can produce large amounts of electricity without creating concern for depletion. However, they have the disadvantage of the amount of electricity obtained being highly dependent on the climatic conditions and time of day. Finding a renewable energy source that can constantly supply the necessary amount of electricity without being influenced by weather or time is urgently needed.

Salinity gradient energy (SGE) is a promising option for meeting these demands. SGE is renewable energy produced by mixing two types of aqueous solutions: freshwater flowing into rivers and salt water into the sea [4]. Hence, SGE can be collected from near estuaries at any time, that is, regardless of the climate or time of day, and there is no concern regarding depletion. Pressure-retarded osmosis (PRO) is a well-established process used for extracting SGE [5,6]. The PRO mechanism is based on the principle that, when two solutions with different salinities are separated by a semipermeable membrane, only water molecules permeate in one direction, from river water to seawater (Fig. 1). This one-way infiltration causes a volumetric increase in the seawater compartment, after which injecting the diluted seawater into rotating turbines enables electricity generation [7]. In addition to PRO, multiple other techniques, such as reverse electrodialysis (RED) [8–10] and capacitive mixing (CapMix) [11–13], have been well-established for the extraction of SGE by controlling the ion conduction in mixed solutions [9,12–19]. Differences between the three techniques are summarized in Table 1. For more details, readers can refer to Refs. [20–26] on the science of SGE and Refs. [27–30] on the latest technological advances.

Theoretically, the electric power obtained from the global SGE potential has been estimated to be 1 TW or more [31–35], which is comparable to the global solar and wind energy consumption [36]. From a local perspective, the SGE potential at the country scales [37–44] and those at regional scales [45–54] have been assessed, where the

* Corresponding author.
E-mail address: hshima@yamanashi.ac.jp (H. Shima).

https://doi.org/10.1016/j.desal.2025.118706
Received 12 December 2024; Received in revised form 23 January 2025; Accepted 16 February 2025
Available online 20 February 2025

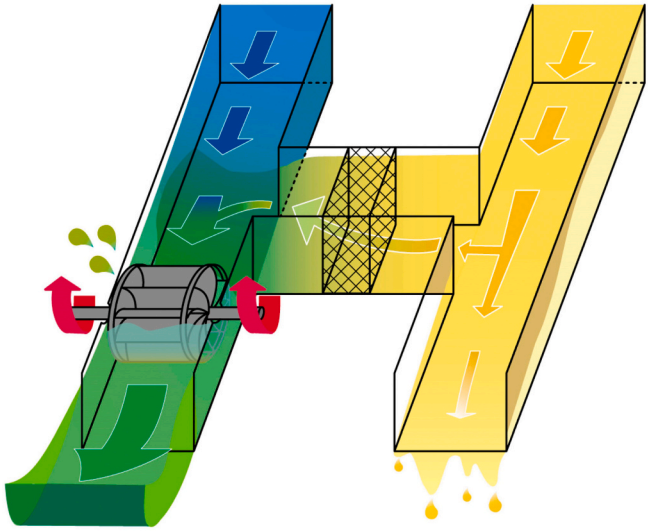

Fig. 1. Mechanism of salinity gradient power (SGP) generation. Water molecules contained in fresh water (colored in yellow) pass through a semipermeable membrane (hatched portion in the center), increasing the water volume in the salt water side (colored in blue). The resulting salt water with increased volume and diluted salinity (colored in green) is spouted to rotate a turbine and generate electricity.

calculation method and the precise definition of the SGE potential has varied depending on the study. A common idea when considering the SGE potential is that the more river water available, the more electrical power can be generated. This indicates that SGE application is suitable for estuaries that have rivers with high flow rates, that is, having a large volume of water passing through the cross-section of the river per unit time.

In view of the discussion above, the coastal areas in Japan are expected to be suitable for salinity gradient power (SGP) generation. Japan is a long and narrow island country with four large islands aligned from north to south, and approximately three-quarters of the land is occupied by forests and mountains. Despite its small land area, Japan's annual rainfall (ca. 1700 mm/year) is nearly twice the global average (ca. 880 mm/year), leading to an increase in the river flow rate. Furthermore, most rivers in Japan are shorter and have steeper slopes than those in other large continental countries. Hence, SGP generation will be optimized in Japan by utilizing the abundant river water flowing into estuaries. However, to the best of our knowledge, no study has calculated the SGE potential in the coastal areas of Japan.

In the present study, the first analysis of the SGP theoretically available in estuaries in Japan was conducted. We focused on the 109 first-class water systems that flow through Japan (see Appendix A); we then considered the daily flow rate changes in each water system and calculated the amount of electric power that could be obtained from the estuaries. Based on the results, we identified Japan's most favorable locations for SGE harvesting, followed by a comparison of the SGE potential in Japan with those in other countries.

2. Method

2.1. Thermodynamic interpretation of SGE

SGE is defined as the energy that can be extracted from the controlled mixing of seawater and river water. From a thermodynamic perspective, the amount of SGE is equal to the reduction in Gibbs free energy caused by using a mixing process [56,57]. The mixing-induced reduction in Gibbs free energy, denoted by $\Delta G_{\mathrm{mix}}(<0)$, can be expressed mathematically as follows:

Table 1
Comparison of the three SGP generation methods.

Method	Main apparatus	Operation mechanism	References
Pressure-Retarded Osmosis (PRO)	Semipermeable membrane (allowing only water molecules to pass through)	PRO is a technology that uses the osmotic pressure created between two solutions of different concentrations. Due to the forwarded osmosis across the semipermeable membrane, the volume of the high concentrated solution increases, and the resulting enhanced water flow is used to rotate a turbine to generate electricity.	Refs. [5,6]
Reverse Electrodialysis (RED)	Cation exchange membrane (allowing only positive ions to pass through), Anion exchange membrane (allowing only negative ions to pass through)	RED is a technology that extracts energy through selective ion permeation and spontaneous redox reactions. Positive and negative ion-exchange membranes are alternately arranged, and solutions of different concentrations are alternately stored in the gaps between the membranes. The potential difference between the electrodes at both ends then causes a redox reaction, which generates an electric current throughout the circuit.	Refs. [8–10]
Capacitive Mixing (CapMix)	Porous electrode (e.g., Activated carbon with high specific surface area)	CapMix is a technology that uses the salinity gradient at the interface between the electrode and the electrolyte to extract a potential difference. A pair of porous electrodes are inserted into the electrolyte; after then, charge-discharge switching and solution flow in-out switching are cyclically repeated to acquire capacitive energy produced by the expansion of the electric double layer.	Refs. [11–13]

$$\Delta G_{\mathrm{mix}} = G_m - (G_s + G_r), \tag{1}$$

where G_m is the Gibbs free energy of the mixed water, while G_s and G_r are the Gibbs free energies of seawater and river water prior to mixing, respectively.

An order estimation of $|\Delta G_{\mathrm{mix}}|$ can be captured by assuming that 1 m^3 of fresh river water (5×10^{-3} mol/L NaCl) is mixed with 1 m^3 of seawater (0.5 mol/L NaCl). In that situation, $|\Delta G_{\mathrm{mix}}|$ is approximately 1.8 MJ ($\simeq$ 0.5 kWh) under ambient conditions [58]. This energy is nearly equal to the hydroelectric (kinetic) energy obtained from depositing a 1 m^3 block of water from the top of a 40-story high-rise building with height of 180 m. Otherwise, if 1 m^3 of fresh river water

flows into the ocean with an infinitely large amount of salt water, approximately 2.7 MJ (≃ 0.75 kWh) of energy will be dissipated into the ocean [41,59,60]. This brief explanation helps readers understand the energy scale provided by SGP generation.

2.2. SGP evaluation formula

For practical use in estimating SGE values, each term in Eq. (1) should be rewritten as a function of the amount of dissolved components, the temperature and volume of the solution, and other factors. This is achieved by transforming Eq. (1) to the following expression [61,62]:

$$P_{SG} = 2RTQ\left[C_s ln\left(\frac{2C_s}{C_s + C_r}\right) + C_r ln\left(\frac{2C_r}{C_s + C_r}\right)\right]. \quad (2)$$

Here, P_{SG} [W] is the SGP, that is, the energy that can be extract from a mixed solution per unit time. In Eq. (2), R [J/(K·mol)] is the universal gas constant, T [K] is the water temperature, and Q [m^3/s] is the river flow rate that determines the volume of fresh water available per unit time for power generation. C_s and C_r [mol/m^3] are the molar concentrations of salt in seawater and river water, respectively. See Appendices B and C for detailed derivations of Eq. (2). Regarding the seawater required for power generation, it was assumed that the same volume of seawater as that of river water could be freely obtained from the sea.

Eq. (2) indicates that, considering an estuary on the coast of Japan, the following four parameters are required to calculate the SGP: Q, T, C_s, and C_r. Among these four parameters, the annual average values of the last three parameters show no major differences between years, while they fluctuate slightly depending on the location of the estuary. The measured values of these three parameters near the estuaries were obtained from "The National Atlas of Japan", published by the Geospatial Information Authority of Japan [63]. In contrast, the annual average value of Q differs significantly among estuaries and measurement years. The next two sections explain the calculation of the annual mean river flow, Q, for estuaries, each belonging to a different water system.

2.3. First-class water systems in Japan

Fig. 1 shows the spatial distribution of the main river channels, consisting of the 109 first-class water systems and relevant watershed boundaries [55]. In Fig. 2(a), only rivers with upstream areas of 500 km^2 or greater are depicted, and rivers with upstream areas of 1500 km^2 or more are highlighted using thick lines. Solid red circles located along the coastline indicate the locations of the estuaries associated with each of the 109 water systems. Domains drawn in Fig. 2(b) illustrate the configuration of the catchment areas of the 109 water systems. The total catchment area over the 109 water systems covers 65 % of the land in Japan [64].

For all estuaries marked in Fig. 2, we obtained daily flow change data for the past 11 years (2012−2022). The data were obtained from a database published by the Ministry of Land, Infrastructure, Transport and Tourism [65]. To calculate river flow in the estuaries, the gauging stations with the fewest missing data points were selected from the most downstream stations in each water system. The observed flow at that station, catchment area upstream of that station, and area of the entire basin were then used to calculate the flow in the estuaries of the river. Fig. 3(a) shows an example of the daily change in the river flow rate, Q [m^3/s], in the estuaries of the Shinano River and Kiso River, belonging to

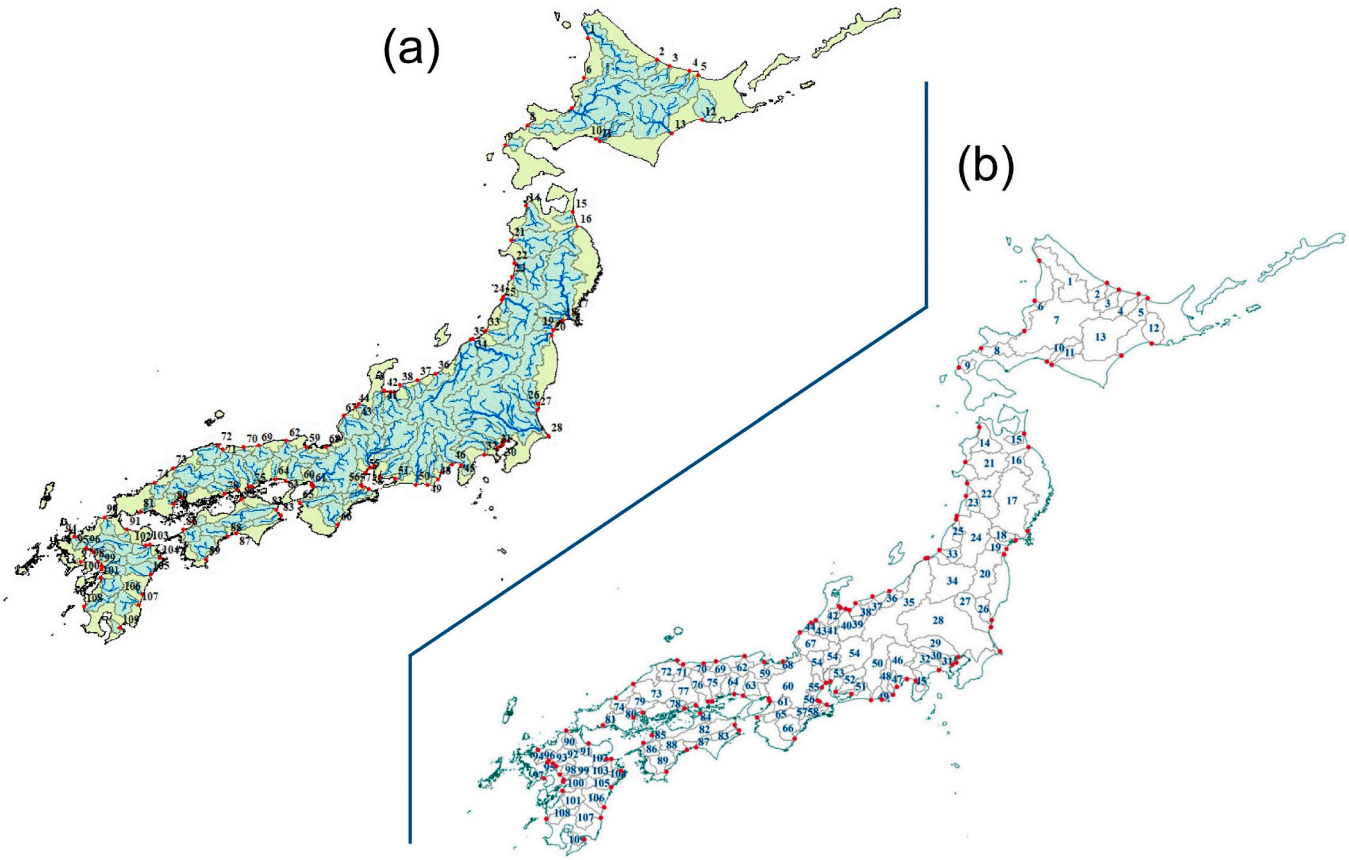

Fig. 2. (a) River channels (branched blue lines) and watershed boundaries (light-blue domains) of 109 first-class water systems located in Japan [55]. (b) Diagram that makes it easier to understand the watershed area of each water system. Red dots aligned along the shoreline indicate the location of the estuary associated with each water system. Numeric labels attached to the estuaries in panel (a) and to the domains in panel (b) correspond to the specific names of the rivers listed in Table 2.

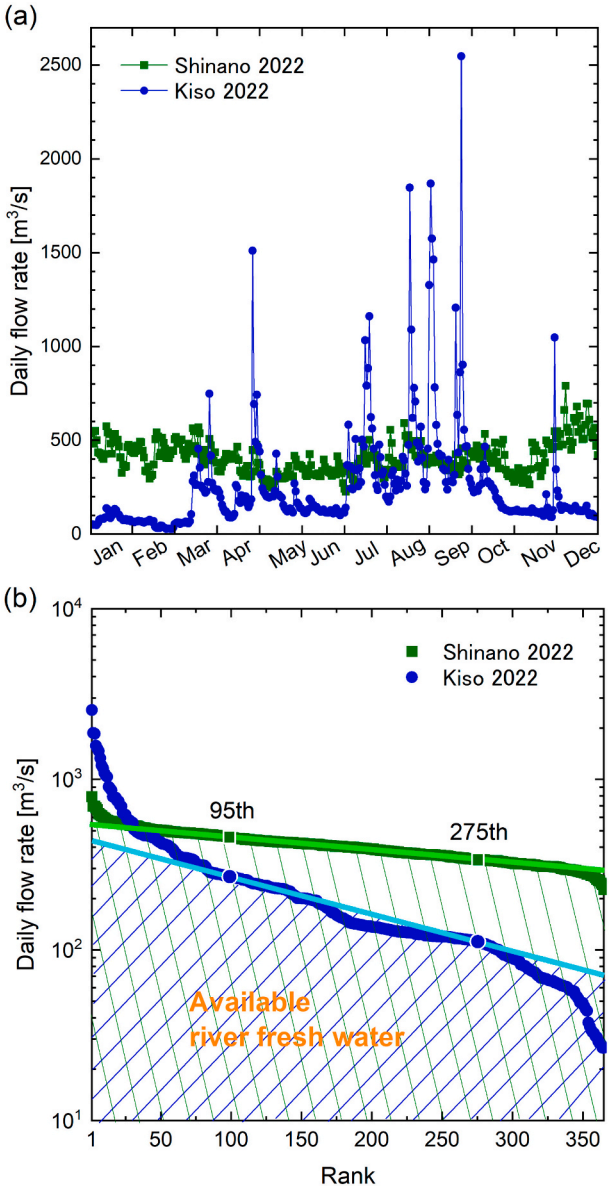

Fig. 3. (a) Time-series data on the daily flow rate of the Shinano River and Kiso River (labeled by 35 and 54 in Fig. 2, respectively) in 2022. (b) Flow duration curve of the two rivers in 2022. The 95-day flow and 275-day flow are marked by points. The area of the trapezoid indicated by the shaded area below the straight line accounts for the amount of water that can be taken into an SGP generation plant in a year.

first-class water systems located in Japan (labeled by 35 and 54 in Fig. 2 (a), respectively), for 2022. The graph shows that the flow rate fluctuated considerably every day. Especially for Kiso River, the flow rate around April and August–September in 2022 increased intermittently because of sudden heavy rainfall associated with approaching typhoons, whereas such the intermittent increase is not found in the data of Shinano River in 2022. As can be inferred from Fig. 3(a), the degree of flow rate fluctuation and the presence or absence of intermittent flow increases vary greatly from river to river and observation years.

2.4. Analysis of river flow rate

In principle, the total amount of water obtainable from a river for using SGP generation can be evaluated by numerically integrating the daily time-series flow-rate curve (as demonstrated in Fig. 3(a)) from end to end and quantifying the area between the curve and the horizontal axis. However, this integration-based method requires considerable effort to obtain the latest 11-year average of the flow rate for each of 109 estuaries. Such a brute-force approach requires the examination of a large amount of data for daily river flow rate. Instead of such a laborious one, we developed the following alternative approach, as explained below, based on the flow duration curve. Regarding terminology, a flow duration curve refers to a curve drawn by sorting daily data on the flow rate observed throughout a year, in descending order.

Fig. 3(b) shows the flow duration curve for the Kiso River, where the daily river flow rates within one year are arranged in descending order from left to right. The vertical axis of the graph is plotted on a logarithmic scale. In general, the flow duration curve tends to have a gentle downward slope toward the right, which visually depicts the degree of change in the river flow rate and the abundance of flow in a year. In Japan, the following four indicators are conventionally used to characterize the shape of flow duration curves: 95-day (25 %) flow, 185-day (50 %) flow, 275-day (75 %) flow, and 355-day (97 %) flow. Here, 95-day flow refers to the 95th largest flow rate from the top, indicating a daily natural flow rate with a probability of exceedance of approximately 25 %. Similar definitions apply to the other three indicators with different threshold days and probabilities. In Japan, these four indicators are measured annually for all major domestic rivers, and they are published on the Internet.

An important observation in Fig. 3 is that the river flow rate data points can be approximated using a straight line downward toward the right within the intermediate region sandwiched by the 95-day and 275-day flows, both of which are marked by arrows in Fig. 3(b). Using this approximately straight line, we can easily determine the amount of water that can be withdrawn, indicated by the shaded area in the graph. Specifically, only the two indicator values have to be selected from a database for a given river and year. The trapezoidal area is below the straight line, which can be easily calculated from the two indicator values, is nearly equal to the amount of water that can be taken in in one year, from which the annual mean Q of the river flow rate can be evaluated. Incidentally, our approach ignores the contribution from the peak located in the upper left-hand corner of the flow curve, that is, the contribution from the few days when the river flow is significantly above the annual average. However, in practice, it is difficult to effectively use such suddenly swollen river water for SGP generation; therefore, this method of ignoring its contribution is appropriate. In the actual analysis, we calculated the SGP of each river by substituting the latest 11 year-average values of the flow rate for all 109 estuaries as Q [m^3/s] in Eq. (2).

2.5. Environmental and technical constraints

Provided that all the river flows determined in the previous section can be used for power generation, the electric power expressed by Eq. (2) can be ideally obtained. In the actual operation of SGP generation, however, it is mandatory that a certain degree of flow in the riverbed remains after water intake to reduce harmful impacts on the ecology, circulation, and sediment transport of the water systems [48,66]. In other words, only a limited fraction of river flow can be used in power generation plants to satisfy environmental demands. According to the well-known Tennant criteria [67], 70 % of river flow can generally be taken from a river. However, from a practical viewpoint, we believe that the inconveniences associated with water extraction cannot be avoided without more stringent restrictions on the percentage of water intake. In addition, when determining the amount of water to be taken from a river in Japan, negotiations with water rights holders tend to be never easy because of a complicated web of interests between parties. As a result, the water withdrawal conditions that must be met by the developer vary widely from river to river, sometimes imposing very strict conditions. Considering such the circumstances unique to Japan, we assumed that, in the present study, only 10 % of the river flow could be utilized for SGP

generation, with the remaining 90 % being the residual river flow after extraction. The reason why we assumed the severe water withdrawal conditions was to avoid overestimating the amount of available SGP by optimistic bias. Nevertheless, this severe condition could be further improved if we had abundant information and more knowledge on the site-specific environmental impacts on each estuary considered, though the presented methodology will serve as an indicative reference for SGP potential assessment under severe intake-flow limitations.

We also considered the constraints on energy conversion in the SGP generation process due to technical limitations. Eq. (2) assumes 100 % efficiency of energy conversion from physico-chemical energy to electric energy. However, in actual PRO (and other) processes, a certain portion of energy is unavoidably dissipated, and the amount of power obtained varies remarkably depending on the performance of the semipermeable membrane. In this study, the technical constraints on SGP generation were considered by referring to detailed analyses of PROs reported previously [59] and assuming an energy conversion efficiency of 40 %, following the literature.

In the following section, we distinguish between the two classes of SGPs: The first is the ideal electric power, calculated based on 100 % river water consumption and 100 % energy conversion efficiency, which we will refer to as the "theoretical" SGP. The other is the realistic electric power, calculated by considering environmental and technical constraints, which we will refer to as the "practical" SGP.

3. Results and discussions

3.1. Domestic distribution of SGE potential

Table 2 summarizes the numerical results of the SGP values at estuaries belonging to the 109 first-class water systems in Japan. The indices attached to the names of the rivers correspond to those shown in Fig. 2. The abbreviation "Theor." denotes the theoretical SGP, and "Pract." denotes the practical SGP. Large values of SGP are highlighted in bold. The total and average SGP values for Japan are listed at the bottom right of the table.

A comparison of the map in Fig. 2 with Table 2 shows that, among the top seven estuaries, the three with the highest SGP values (labeled 24, 34, and 35) are concentrated in the northern part of the coast of the Sea of Japan. A possible reason for this is that the annual precipitation in this region is higher than that in other regions, which increases the river flow rate in estuaries. In addition, the sum of SGP values for the top seven estuaries (shown in bold) account for more than 33 % of the total SGP values over the all 109 water systems, which suggest suitable sites for the introduction of SGP facilities. The results in Table 2 provide basic information for considering the construction of SGE power generation facilities in Japan in the future.

3.2. Comparison of power output by generation method

Table 3 compares the SGP values expected for Japan and the electric power that can be generated using other power generation methods in Japan. The two columns on the left show the average and maximum amount of power that can be generated per power plant. The rightmost column shows the total amount of power that can be generated by all the power plants in the country. An important finding in Table 3 is that, despite of the severe restriction regarding the water intake ratio and energy conversion efficiency we have assumed, the practical SGP per plant is not by far smaller than the power produced via solar, wind, and other renewable-type power generation (as highlighted by bold in Table 3). This indicates that SGE can be used as a major renewable energy resource in the future, similar to solar and wind power. As mentioned previously, solar and wind power generation have the following disadvantages: They depend weather conditions and the time of day. Therefore, using SGE in a complementary manner to compensate for this weakness may make it possible to increase the rate of energy supply from renewable sources in Japan.

Table 4 demonstrates the operational experience for marine energy power generation in Japan. All the results are from the trial phase, and there are no examples of social implementation yet. The SGE value shown in the table is for power plants that were under construction at the time of writing this article (scheduled to be operational in 2025; see Section 3.6). The extent to which these marine-based renewable energies can be effectively operated and developed is a key issue for maritime countries such as Japan.

3.3. SGP comparison by country

Table 5 compares the SGP of Japan (calculated in this study) with those expected in other countries. The theoretical SGPs listed in the leftmost column were evaluated under the assumption that that all river flows could be utilized. The practical SGPs listed in the middle column were evaluated for various countries by imposing certain restrictions on the available river water volume and energy conversion efficiency. It should be noted that, however, the restriction criteria differ depending on the study; therefore, it is not possible to simply compare the practical SGPs presented in the table. The table also shows in the rightmost column the theoretical SGP divided by the country's land area. An interesting finding is that the theoretical SGP per unit land area was significantly higher in Japan than in other countries. This result is due to the fact that rivers with sufficient flow are widely distributed throughout Japan, and it supports the suitability of SGP power generation for Japan.

3.4. SGP comparison by major rivers worldwide

Table 6 shows SGP comparisons of major rivers worldwide. In the upper rows of the table, the seven rivers in Japan with the highest practical SGP values are shown. The lower rows show examples of SGP values calculated for rivers in other countries in previous studies. The order of the river (or estuary) names in the table follows the estimated power divided by the basin area of each river, as shown in the leftmost column in the table. Focusing on the values in this leftmost column, the SGPs per basin area, reveals an interesting geographic feature of Japan as explained below. For instance, the practical SGPs per basin area for ChangJing River in China and Ganges River in Bangladesh account for 6.0 kW/km^2 and 1.3 kW/km^2, respectively, which are of the same order of the practical SGPs per basin area for Japan's rivers such as 3.4 kW/km^2 in Shinano River and 3.6 kW/km^2 in Kiso River. Recalling that the first two are both huge world-class rivers and the latter two are smaller one, it should not be trivial that the SGPs per basin area are the same order for all those rivers. In fact, the practical SGPs for ChangJing River and Ganges River are more than 11,000 MW and 2000 MW, respectively; these values are two or three magnitudes higher than the SGP of Japanese rivers. Nevertheless, the practical SGP values per basin area were found to be around the same. This result implies that in Japan, the flowing water collected within a relatively small basin can be used efficiently as an energy source for SGP power generation. This unique situation stems from the country's unique geographical characteristics, which include many mountains, forests, and steep slopes.

3.5. Technical limitations on SGP output

As described in Introduction, there are three main methods to acquire SGE. A question that naturally arises would be which method is the most promising. On the issue, different researchers may have different opinions. Nevertheless, many seem to agree that PRO is closest to entering the social implementation phase. For example, the quantitative and thorough analysis reported in Ref. [73] concluded that PRO has theoretical properties that exceed RED and CapMix in both energy conversion efficiency and membrane power density. This is a reason why we applied the energy conversion efficiency (ca. 40 %) that had been evaluated for the PRO mechanism in Ref. [59].

Table 2
SGP obtained in estuaries belonging to different water systems. "Theor.[MW]" means the theoretical SGP, defined by the extractable power under the assumptions of 100 % river-water consumption and 100 % energy conversion efficiency. "Pract.[MW]" means the practical SGP, which is expected when assuming a restriction of only 10 % river-water consumption and 40 % energy conversion efficiency. The seven rivers with the highest output are shown in bold. Where more than one river has the same name, the relative location of the river located to the east or west (or north or south) is specified in parentheses.

Index	River's Name	Theor. [MW]	Pract. [MW]	Index	River's Name	Theor. [MW]	Pract. [MW]	Index	River's Name	Theor. [MW]	Pract. [MW]	Index	River's Name	Theor. [MW]	Pract. [MW]
1	Teshio	380	15.2	29	Ara(south)	108	4.3	57	Kushida	30	1.2	85	Shigenobu	21	0.9
2	Shokotsu	58	2.3	30	Tama	46	1.8	58	Miya	51	2.0	86	Hiji	49	2.0
3	Yubetsu	54	2.2	31	Tsurumi	30	1.2	59	Yura	103	4.1	87	Monobe	37	1.5
4	Tokoro	51	2.0	32	Sagami	92	3.7	60	Yodo	405	16.2	88	Niyodo	136	5.5
5	Abashiri	37	1.5	33	Ara(north)	209	8.3	61	Yamato	40	1.6	89	Watari	415	16.6
6	Rumoi	14	0.6	**34**	**Agano**	**729**	**29.2**	62	Maruyama	80	3.2	90	Onga	53	2.1
7	**Ishikari**	**993**	**39.7**	**35**	**Shinano**	**998**	**39.9**	63	Kako	62	2.5	91	Yamakuni	18	0.7
8	Shiribetsu	114	4.6	36	Seki	129	5.2	64	Ibo	46	1.9	92	Chikugo	177	7.1
9	Shiribeshitoshibetsu	75	3.0	37	Hime	71	2.8	65	Kino	121	4.9	93	Yabe	29	1.1
10	Mu	69	2.7	38	Kurobe	29	1.2	66	Shingu	219	8.8	94	Matsuura	22	0.9
11	Saru	81	3.2	39	Jyoganji	29	1.2	67	Kuzuryu	483	19.3	95	Rokkaku	13	0.5
12	Kushiro	137	5.5	40	Jinzu	184	7.4	68	Kita	20	0.8	96	Kase	37	1.5
13	Tokachi	459	18.4	41	Sho	84	3.4	69	Sendai(north)	101	4.0	97	Honmyou	16	0.7
14	Iwaki	195	7.8	42	Oyabe	116	4.7	70	Tenjin	37	1.5	98	Kikuchi	54	2.1
15	Takase	62	2.5	43	Tedori	150	6.0	71	Hino	45	1.8	99	Shira	37	2.1
16	Mabechi	88	3.5	44	Kakehashi	50	2.0	72	Hii	162	6.5	100	Midori	70	2.8
17	**Kitakami**	**702**	**28.1**	45	Kano	89	3.5	73	Gono	203	8.1	101	Kuma	154	6.1
18	Naruse	86	3.4	46	Fuji	172	6.0	74	Takatsu	80	3.2	102	Oita	39	1.6
19	Natori	54	2.2	47	Abe	47	1.9	75	Yoshii	111	4.4	103	Ono	74	3.0
20	Abukuma	200	8.0	48	Oi	86	3.4	76	Asahi	85	3.4	104	Banjo	17	0.7
21	Yoneshiro	348	13.9	49	Kiku	15	0.6	77	Takahashi	98	3.9	105	Gokase	148	5.9
22	Omono	410	16.4	50	Tenryu	373	14.9	78	Ashida	32	1.3	106	Omaru	57	2.3
23	Koyoshi	164	6.6	51	Toyo	37	1.5	79	Ota	126	5.1	107	Oyodo	253	10.1
24	**Mogami**	**570**	**22.8**	52	Yahagi	76	3.0	80	Oze	20	0.8	108	Sendai(south)	164	6.6
25	Aka	148	5.9	53	Shonai	53	2.1	81	Sabe	23	0.9	109	Kimotsuki	51	2.1
26	Kuji	45	1.8	**54**	**Kiso**	**826**	**33.0**	82	Yoshino	195	7.8				
27	Naka(east)	177	7.1	55	Suzuka	15	0.6	83	Naka(west)	89	3.6		Total	16,518	660.7
28	**Tone**	**669**	**26.8**	56	Kumozu	25	1.0	84	Doki	3	0.1		Mean	152	6.1

Table 3
Comparison of the electric power output obtained using different power generation methods in Japan. The SGP values were evaluated for the 109 domestic estuaries in the present study. In addition, the power generation capacity (i.e., the maximum amount of power that a generator can produce when running at full performance) for existing power plants were presented. Numerical data other than those of SGP were obtained from the database of METI Agency for Natural Resources and Energy.

	Average output [MW/plant]	Maximum output [MW/plant]	Number of plants existed	Total output in Japan [GW]
SGP (Theor.)	152	998	109	16.5
SGP (Pract.)	**6**	**40**	109	6.6
Nuclear	2206	8212	15	33.1
Thermal	336	5160	467	15.6
Biomass	50	4100	98	4.6
Hydro	**28**	**560**	1674	49.5
Geothermal	**26**	**112**	17	0.4
Wind	**13**	**122**	356	4.6
Solar	**4**	**258**	4724	16.4

Table 4
Marine energy power generation conducted in Japan. All outputs are a result of the trial phase, and there are no examples of social implementation yet.

	Operation year	Output [kW]	Reference
SGP	(2025-)	110	Ref. [68]
Wave	2015-	100	Ref. [69]
Tidal current	2021-	500	Ref. [70]
Ocean current	2019–2021	100	Ref. [71]
Ocean thermal	2022-	100	Ref. [72]

Table 5
Comparison of the total SGP over the entire national land area (or the region for Québec in Canada) with the SGP per land area. Note that the method of calculating Pract. values differs depending on the study.

	Theor.total [MW]	Pract.total [MW]	Theor. Per land area [kW/km^2]	Reference
Japan	16,518	661	34.7	Present work
Colombia	15,629	n/a	13.7	Ref. [43]
USA	120,000	n/a	12.2	Ref. [37,41]
Norway	2854	n/a	7.4	Ref. [38]
Sweden	2611	1825	5.8	Ref. [44]
China	40,271	22,454	4.2	Ref. [39]
Québec	n/a	5222	n/a	Ref. [40]

It should be emphasized, however, that other technical issues must also be considered for considering the realistic operational feasibility of SGP generation. An important issue inherent to SGE harvesting is a trade-off between efficiency and power [60]. First, the slower the rate of power generation, the better the efficiency of power generation; this is because a larger fraction of the Gibbs energy in solution is converted to mechanical energy in the water flow with higher efficiency. However, in this case, the power (i.e., energy obtained per unit time) is smaller because less water passes through the semipermeable membrane per unit time. Conversely, to increase the power obtained, we have only to pass a large volume of water quickly across the membrane. In this case, however, most of the Gibbs energy is dissipated, so the conversion efficiency is smaller. Analysis of the most favorable conditions for resolving this trade-off has shown that the maximum power obtained drops to half to a fraction of the value shown in Eq. (2) [73].

Another important factor that reduces the SGP available in reality is the energy loss associated with pumping operations to maintain water flow and the pretreatment of the solution required to remove foulants (e.g., colloids and biofilm-forming microbes). The energy costs of pumping and pretreatment are proportional to the volume of solution entering the SGP plant. Therefore, these energy costs should be subtracted when estimating the net output of the plant. In addition, restricted mass transport within the support layer is critical to PRO performance. The porous support layer used in PRO serves to protect the membrane from water flow and pressure, but it also acts as an unstirred boundary layer

Table 6
SGP comparison by major rivers in the world. The numbers marked with # coincide with the numbers of each river shown in Fig. 2 and Table 2. The superscripts *, **, *** mean that the numeric data involve yearly, seasonal, and scenario-derived variation, respectively, and thus a single value of SGP cannot be deduced from the reference.

	Power. Per basin area [kW/km^2]	Power [MW]	Basin area [km^2]	Reference
Agano (#34)	3.8	29.2	7710	Present work
Kiso (# 54)	3.6	33.0	9100	Present work
Shinano (# 35)	3.4	39.9	11,900	Present work
Mogami (# 24)	3.2	22.8	7040	Present work
Ishikari (# 7)	2.8	39.7	14,330	Present work
Kitakami (# 17)	2.8	28.1	10,150	Present work
Tone (# 28)	1.6	26.8	16,840	Present work
[Theor.]				
BonsSinais Estuary (Mozambique)	56.9	1086.8	19,104	Ref. [53]
Incomati Estuary (Mozambique)	18.1	843.6	46,725	Ref. [53]
Göta River (Sweden)	17.4	896.0	51,489	Ref. [44]
Limpopo Estuary (Mozambique)	3.2	1292.0	407,137	Ref. [53]
Zambezi River (Mozambique)	2.0	2800.0	1,377,869	Ref. [53]
[Pract.]				
Sebou Estuary (Morrocco)*	1.7–34.5	65.0–1303.0	37,813	Ref. [51]
Sebou Estuary (Morrocco)**	0.3–11.4	12.25–430.5	37,813	Ref. [54]
León River (Colombia)	6.5	14.2	2186	Ref. [48]
ChangJing River (China)	6.0	11,537.0	1,909,199	Ref. [39]
Muthupet Estuary (India)**	0.0–2.2	0.0–175.2	78,368	Ref. [54]
Ganges River (Bangladesh)	1.3	2080.0	1,574,223	Ref. [41]
Columbia River (USA)	1.2	780.0	651,407	Ref. [41]
Ceyhan River (Turkey)	1.1	24.0	21,249	Ref. [50]
Strymon River (Greece)	0.7	11.0	16,801	Ref. [52]
Brisbane River (Australia)	0.7	10.0	13,651	Ref. [42]
Mississippi River (USA)	0.6	1870.0	3,179,311	Ref. [41]
Meric River (Turkey)	0.6	30.0	52,512	Ref. [50]
Sakarya River (Turkey)	0.4	23.0	62,799	Ref. [50]
[Hyper saline lake]				
ZarrinehRud River (Iran)	21.3	310.8	14,587	Ref. [49]
Dead Sea(Jordan-Israel)***	1.8–2.6	48.3–70.5	27,336	Ref. [46]
Great Salt Lake (USA)	0.8	66.3	86,895	Ref. [47]

that prevents adequate mixing of the solution. As a result of this side effect (known as concentration polarization), excess solutes accumulate inside the membrane, reducing the driving force of water permeation. Thus further innovations of the membrane support layer morphology are desired to attain more efficiency in PRO performance. Detailed and critical reviews on this issue have been reported as Refs. [23,26].

3.6. SGE development trend in Japan

Before concluding the article, we will briefly touch on domestic trends in SGE technology development in Japan. Regarding PRO technology, a national project called Mega-ton Water System Project was conducted during 2009–2013 [74–76]. This project considered the use of concentrated seawater from desalination plants and treated sewage water for PRO power generation, as alternatives to seawater and river water. As a result of promoting the project, an increase in power output was expected, and the prospect of practical application of PRO power generation was achieved. It was also estimated that by incorporating SGP generation equipment into existing seawater desalination facilities, up to 10 % of the facility's electricity consumption could be generated. Currently, Kyowakiden Industry Co., Ltd. is installing a PRO system at a seawater desalination facility in Fukuoka City (located in southern Japan), with the aim of commercializing the system in 2025 [77].

In view of device development, Toyobo Co., Ltd. is leading the field as the sole developer of commercial PRO membranes [78]. In a PRO demonstration test initiated in 2018 by the Danish venture Salt Power Aps, Toyobo's membranes were used to successfully generate 20 kW of electricity. For RED components, the Blue Energy center for SGE Technology (BEST), a research center established at Yamaguchi University in 2018, successfully developed a large RED stack with the world's largest membrane area in 2019 and evaluated its power output [79]. In a maritime country of Japan, it is expected to make further progress in SGE development from the perspectives of both elemental technology and facility design.

4. Summary

In this study, we quantified the SGP that could be extracted from each of Japan's 109 major rivers, using a publicly available river flow database. The results showed that areas with high SGP values were concentrated on northwestern side of the Sea of Japan. It was also found that the SGP in Japan could be expected to be comparable to or higher than that of electric power based on other types of renewable energy in operation. This result indicated that, by combining SGP power generation with solar and wind power generation, SGP can be used as a complementary energy source to compensate for the weaknesses of the latter. Furthermore, it was demonstrated that the SGPs that could be obtained per national land area and per basin area were comparable between Japan and other huge continental countries. This is thought to be due to Japan's unique geographical characteristics, including the large number of forests and steep river slopes. We anticipate that this first quantitative analysis of SGP will provide insights into the development of new energy sources in Japan.

CRediT authorship contribution statement

Kotomi Watanabe: Writing – original draft, Conceptualization, Methodology, Data curation, Formal analysis, Investigation, Writing – review & editing. **Yuri Akiba:** Data curation, Software, Writing – review & editing. **Hiroshi Ishidaira:** Methodology, Software, Writing – review & editing. **Hiroyuki Shima:** Writing – original draft, Conceptualization, Methodology, Formal analysis, Investigation, Writing – review & editing, Supervision, Project administration, Funding acquisition.

Declaration of competing interest

The authors declare that they have no known competing financial interests or personal relationships that could have appeared to influence the work reported in this paper.

Acknowledgments

We are thankful for the fruitful discussions with Ms. Keiko Okamoto in GPSS Holdings Inc., Prof. Motohiro Sato in Hokkaido University, Prof. Yoichi Shimazaki and Assoc. Prof. Yoshiyuki Kinose in University of Yamanashi, Ms. Maika M. Hayashi and Asst. Prof. Tadashi Kunieda in Nara Institute of Science and Technology, Ms. Aki Odawara in Osaka University, and Prof. Hideo Yoshioka in Nara Women's University. We also thank Ms. Makiko Toyoura for assisting in producing the illustrations. This work was supported by JSPS KAKENHI, Grant Numbers JP22K19727 (H.S), JP22K04328 (H.I), JP24K17370 (Y.A), and JP24K01111 (H.S).

Appendix A. Terminology

It should be noted that there is a slight difference in the meanings of the following two terminologies: "river" and "water system." In general, rivers are streams of water that flow from sources in mountainous areas, join together upstream, and gradually grow toward the sea as they continue to merge. A water system is a collection of rivers of various sizes (main rivers, tributaries, etc.) from the water sources to the river mouths.

What is called a first-class water system in Japan is a water system that is particularly important from the perspective of preserving national land and protecting people's lives, and that should be managed nationally. In Japan, 109 water systems have been designated as first-class. For all 109 water systems, the annual average river flow rate in estuaries was estimated, followed by an evaluation of the electric power that could be produced from SGE.

Appendix B. Derivation of SGE power formula

Appendix B shows a derivation of Eq. (2), which describes the amount of electric power obtained from mixing of two solutions at different salinities. The derivation starts with considering the mixing-caused variations in the Gibbs free energy of aqueous solutions, which is expressed as follows:

$$\Delta G_{\mathrm{mix}} = G_m - (G_s + G_r). \tag{3}$$

where G_m is the Gibbs free energy of the mixed water, while G_s and G_r are the Gibbs free energies of seawater and river water prior to mixing, respectively.

For simplicity, we assumed that only three types of substances, namely Na^+, Cl^-, and H_2O, were present in the solution before and after mixing. Subsequently, the Gibbs free energy of the kth solution with $k = \{m, s, r\}$ was given by

$$G_k = \sum_{i=\mathrm{Na}^+,\mathrm{Cl}^-,\mathrm{H_2O}} n_{i,k}\ \mu_{i,k}. \tag{4}$$

where $\mu_{i,k}$ is the chemical potential of the ith species contained in the kth solution, and $n_{i,k}$ is the number of moles of the ith species in the kth solution. We set $n_{\mathrm{Na}^+,k} = n_{\mathrm{Cl}^-,k}$ for all the solutions of $k = \{m, s, r\}$, assuming that the salt (NaCl) was completely ionized in water.

If i represents a solvent (H_2O in this case), the chemical potential of the solvent (i) is defined as

$$\mu_i = \mu_i^* + RTlnx_i \quad \text{for solvent } i, \tag{5}$$

where μ_i^* is the chemical potential of pure solvent i and x_i is the molar fraction of solvent i; R is the universal gas constant, and T is the liquid temperature. Eq. (5) is based on Raoult's law for the vapor partial pressure of solvents in sufficiently diluted solutions [56,57]. Otherwise, when i represents a solute (Na^+ or Cl^- in this case), the following is obtained:

$$\mu_i = \mu_i^{\omega} + RTlnx_i \quad \text{for solute } i, \tag{6}$$

where μ_i^{ω} is the chemical potential of solute i in the standard state and x_i is the molar fraction of solute i. Eq. (6) is based on Henry's law for the vapor partial pressure of solutes in sufficiently dilute solutions [56,57]. Substituting Eqs. (4)–(6) into Eq. (3) yields

$$\Delta G_{\mathrm{mix}} = \sum_{i=\mathrm{Na}^+,\mathrm{Cl}^-,\mathrm{H_2O}} \left[(n_{i,s} + n_{i,r})RTlnx_{i,m} - (n_{i,s}RTlnx_{i,s} + n_{i,r}RTlnx_{i,r}) \right], \tag{7}$$

bearing in mind the relationship $n_{i,m} = n_{i,s} + n_{i,r}$ for $i = \{\mathrm{Na}^+, \mathrm{Cl}^-, \mathrm{H_2O}\}$, which indicates that the number of moles of species (i) should be conserved before and after mixing.

Summation with respect to species i in Eq. (7) can be eliminated by considering the following two conditions. First, the contribution of H_2O to ΔG_{mix} should be significantly lower than those of the other two, when the mixing of seawater and river water is considered. This is supported by the typical values of NaCl concentration, 34 g/L in actual seawater and 1 g/L in actual river water. Using these values, the number of moles per cubic meter of seawater, as $(n_{\mathrm{Na}^+,s}) = (n_{\mathrm{Cl}^-,s}) \simeq 1.0 \times 10^3$ mol and $(n_{\mathrm{H_2O},s}) \simeq 5.5 \times 10^4$ mol, resulted in the following molar fractions: $x_{\mathrm{Na}^+,s} = x_{\mathrm{Cl}^-,s} \simeq 0.02$ and $x_{\mathrm{H_2O},s} \simeq 0.98$. As $x_{\mathrm{H_2O},s}$ is nearly equal to unity, its logarithmic value is close to zero. The same holds true for river water. Therefore, the H_2O contribution can be ignored. Second, the contributions of Na^+ and Cl^- to the expressions in square brackets in Eq. (7) are equal because of the assumption that NaCl is completely ionized in water. As a consequence, Eq. (7) can be simplified to

$$\Delta G_{\mathrm{mix}} = 2RT\left[(n_{\mathrm{Na}^+,s} + n_{\mathrm{Na}^+,r})ln(x_{\mathrm{Na}^+,m}) - (n_{Na^+,s})ln(x_{Na^+,s}) - (n_{Na^+,r})ln(x_{Na^+,r}) \right]. \tag{8}$$

For simplicity, we omitted the subscript Na^+ in the subsequent discussion. By substituting Eqs. (21), (22), and (25), which are presented in Appendix C, into Eq. (8), the following is obtained:

$$\Delta G_{\mathrm{mix}} = 2RT[(n_s + n_r)lnx_m - n_s lnx_s - n_r lnx_r] = -2\tau RT\left[V_s x_s ln\left(\frac{x_s}{x_m}\right) + V_r x_r ln\left(\frac{x_r}{x_m}\right) \right]. \tag{9}$$

where V_k is the volume of the kth solution and τ is the total number of moles per cubic meter of salt solution. See details of V_k and τ in Appendix C.

Subsequently, we transformed Eq. (9) from being in terms of x_k to being in terms of the Na^+ molar concentrations, designated as C_s and C_r, in mol/m^3. From the definition of molar concentration, it is clear that

$$C_s = \frac{n_s}{V_s}, \quad C_r = \frac{n_r}{V_r}, \quad C_m = \frac{n_m}{V_m}. \tag{10}$$

Based on Eqs. (21) and (22), which are provided in Appendix C, the first two expressions in Eq. (10) can be rewritten as

$$C_s = \tau x_s, \quad C_r = \tau x_r. \tag{11}$$

In addition, because $V_m = V_s + V_r$ and $n_m = n_s + n_r$, the final expressions in Eq. (10) is as follows:

$$C_m = \frac{C_s V_s + C_r V_r}{V_s + V_r}. \tag{12}$$

Referring to Eqs. (11) and (25), it can be rewritten as follows:

$$C_m = \frac{\tau x_s V_s + \tau x_r V_r}{V_s + V_r} = \tau x_m. \tag{13}$$

Substituting the results of Eqs. (11) and (13) into Eq. (9), we obtain a C_k-based expression for ΔG_{mix} as

$$\Delta G_{\mathrm{mix}} = -2RT\left[V_s C_s ln\left(\frac{C_s}{C_m}\right) + V_r C_r ln\left(\frac{C_r}{C_m}\right) \right]. \tag{14}$$

The target expression in Eq. (2) can be obtained according to Eq. (14) under the condition that $V_s = V_m = V$, that is, by considering a situation in which the amount of water collected from the sea was the same as that collected from the river. The electricity power P_{SG} generated from the salinity gradient is defined as a decrease in Gibbs free energy per unit time Δt. Finally, we obtain the following formula:

$$P_{SG} = \frac{-\Delta G_{mix}}{\Delta t} = 2RT \cdot Q\left[C_s ln\left(\frac{2C_s}{C_s + C_r}\right) + C_r ln\left(\frac{2C_r}{C_s + C_r}\right)\right], \tag{15}$$

where $Q = V/\Delta t$.

Appendix C. Molar fractions and number of moles

The molar fractions of $x_{i,k}$ for seawater and river water ($k = s$ or r) can be written as follows:

$$x_{Na^+,k} = \frac{n_{Na^+,k}}{(n_{Na^+,k}) + (n_{Cl^-,k}) + (n_{H_2O,k})}, \tag{16}$$

$$x_{Cl^-,k} = \frac{n_{Cl^-,k}}{(n_{Na^+,k}) + (n_{Cl^-,k}) + (n_{H_2O,k})}, \tag{17}$$

$$x_{H_2O,k} = 1 - x_{Na^+,k} - x_{Cl^-,k}. \tag{18}$$

Notably, under the assumption of complete salt ionization, $n_{Na^+,k} = n_{Cl^-,k}$ holds, indicating that $x_{Na^+,k} = x_{Cl^-,k}$.

For convenience, τ was used to denote the total number of moles per cubic meter of salt solution under ambient conditions. The value of τ was assumed to be independent of the salt content, indicating that particles Na^+, Cl^-, and H_2O could be considered independent molecules that are free from interactions. Using the notation of τ, the total numbers of moles in seawater and river water with volumes V_s and V_r, respectively, are denoted as τV_s and τV_r, respectively. Hence, the following is obtained:

$$\tau V_s = (n_{Na^+,s}) + (n_{Cl^-,s}) + (n_{H_2O,s}), \tag{19}$$

$$\tau V_r = (n_{Na^+,r}) + (n_{Cl^-,r}) + (n_{H_2O,r}). \tag{20}$$

Substituting these into Eqs. (16) and (17) yields

$$\tau V_s\ x_{Na^+,s} = n_{Na^+,s}, \tag{21}$$

$$\tau V_r\ x_{Na^+,r} = n_{Na^+,r}. \tag{22}$$

Similarly, the molar fractions of mixed water $k = m$ are expressed as follows:

$$x_{Na^+,m} = \frac{(n_{Na^+,s}) + (n_{Na^+,r})}{\sum_{i=Na^+,Cl^-,H_2O} \sum_{k=s,r} (n_{i,k})}, \tag{23}$$

$$x_{Cl^-,m} = \frac{(n_{Cl^-,s}) + (n_{Cl^-,r})}{\sum_{i=Na^+,Cl^-,H_2O} \sum_{k=s,r} (n_{i,k})}. \tag{24}$$

Using the results from Eqs. (19)–(22), these can be simplified as

$$x_{Na^+,m} = \frac{V_s x_{Na^+,s} + V_r x_{Na^+,r}}{V_s + V_r}, \tag{25}$$

$$x_{Cl^-,m} = \frac{V_s x_{Cl^-,s} + V_r x_{Cl^-,r}}{V_s + V_r}. \tag{26}$$

Again, it should be noted that $x_{Na^+,m} = x_{Cl^-,m}$, because $n_{Na^+,k} = n_{Cl^-,k}$.

Data availability

Data will be made available on request.

References

[1] N.L. Panwar, S.C. Kaushik, S. Kothari, Role of renewable energy sources in environmental protection: a review, Renew. Sust. Energ. Rev. 15 (2011) 1513–1524, https://doi.org/10.1016/j.rser.2010.11.037.

[2] O. Ellabban, H. Abu-Rub, F. Blaabjerg, Renewable energy resources: current status, future prospects and their enabling technology, Renew. Sust. Energ. Rev. 39 (2014) 748–764, https://doi.org/10.1016/j.rser.2014.07.113.

[3] E. Dogan, F. Seker, The influence of real output, renewable and non-renewable energy, trade and financial development on carbon emissions in the top renewable energy countries, Renew. Sust. Energ. Rev. 60 (2016) 1074–1085, https://doi.org/10.1016/j.rser.2016.02.006.

[4] B.E. Logan, M. Elimelech, Membrane-based processes for sustainable power generation using water, Nature 488 (2012) 313–319, https://doi.org/10.1038/nature11477.

[5] A. Achilli, A.E. Childress, Pressure retarded osmosis: from the vision of Sidney Loeb to the first prototype installation - review, Desalination 261 (2010) 205–211, https://doi.org/10.1016/j.desal.2010.06.017.

[6] G. Han, S. Zhang, X. Li, T.S. Chung, Progress in pressure retarded osmosis (PRO) membranes for osmotic power generation, Prog. Polym. Sci. 51 (2015) 1–27, https://doi.org/10.1016/j.progpolymsci.2015.04.005.

[7] K. Matsuyama, R. Makabe, T. Ueyama, H. Sakai, K. Saito, T. Okumura, H. Hayashi, A. Tanioka, Power generation system based on pressure retarded osmosis with a commercially-available hollow fiber PRO membrane module using seawater and freshwater, Desalination 499 (2021) 114805, https://doi.org/10.1016/j.desal.2020.114805.

[8] R.E. Pattle, Production of electric power by mixing fresh and salt water in the hydroelectric pile, Nature 174 (1954) 660, https://doi.org/10.1038/174660a0.

[9] R.A. Tufa, S. Pawlowski, J. Veerman, K. Bouzek, E. Fontananova, G. di Profio, S. Velizarov, J.G. Crespo, K. Nijmeijer, E. Curcio, Progress and prospects in reverse electrodialysis for salinity gradient energy conversion and storage, Appl. Energy 225 (2018) 290–331, https://doi.org/10.1016/j.apenergy.2018.04.111.

[10] C. Tristán, M. Fallanza, R. Ibáñez, I. Ortiz, Recovery of salinity gradient energy in desalination plants by reverse electrodialysis, Desalination 496 (2020) 114699, https://doi.org/10.1016/j.desal.2020.114699.

[11] D. Brogioli, Extracting renewable energy from a salinity difference using a capacitor, Phys. Rev. Lett. 103 (2009) 058501, https://doi.org/10.1103/PhysRevLett.103.058501.

[12] D. Brogioli, R. Ziano, R.A. Rica, D. Salerno, O. Kozynchenko, H.V.M. Hamelers, F. Mantegazza, Exploiting the spontaneous potential of the electrodes used in the capacitive mixing technique for the extraction of energy from salinity difference, Energy Environ. Sci. 5 (2012) 9870–9880, https://doi.org/10.1039/c2ee23036d.

[13] R.A. Rica, R. Ziano, D. Salerno, F. Mantegazza, R. van Roij, D. Brogioli, Capacitive mixing for harvesting the free energy of solutions at different concentrations, Entropy 15 (2013) 1388–1407, https://doi.org/10.3390/e15041388.

[14] J.W. Post, H.V. Hamelers, C.J. Buisman, Energy recovery from controlled mixing salt and fresh water with a reverse electrodialysis system, Environ. Sci. Technol. 42 (2008) 5785–5790, https://doi.org/10.1021/es8004317.

[15] J.G. Hong, B.P. Zhang, S. Glabman, N. Uzal, X.M. Dou, H.G. Zhang, X.Z. Wei, Y. S. Chen, Potential ion exchange membranes and system performance in reverse electrodialysis for power generation: a review, J. Membr. Sci. 486 (2015) 71–88, https://doi.org/10.1016/j.memsci.2015.02.039.

[16] Y. Mei, C.Y.Y. Tang, Recent developments and future perspectives of reverse electrodialysis technology: a review, Desalination 425 (2018) 156–174, https://doi.org/10.1016/j.desal.2017.10.021.

[17] J. Moreno, S. Grasman, R. van Engelen, K. Nijmeijer, Upscaling reverse electrodialysis, Environ. Sci. Technol. 52 (2018) 10856–10863, https://doi.org/10.1021/acs.est.8b01886.

[18] X. Liu, M. He, D. Calvani, H. Qi, K. Gupta, H.J.M. de Groot, G.J.A. Sevink, F. Buda, U. Kaiser, G.F. Schneider, Power generation by reverse electrodialysis in a single-layer nanoporous membrane made from core-rim polycyclic aromatic hydrocarbons, Nat. Nanotechnol. 15 (2020) 307–312, https://doi.org/10.1038/s41565-020-0641-5.

[19] Y. Jiao, C. Yang, W. Zhang, Q. Wang, C. Zhao, A review on direct osmotic power generation: mechanism and membranes, Renew. Sust. Energ. Rev. 191 (2024) 114078, https://doi.org/10.1016/j.rser.2023.114078.

[20] Z.J. Jia, B.G. Wang, S.Q. Song, Y.S. Fan, Blue energy: current technologies for sustainable power generation from water salinity gradient, Renew. Sust. Energ. Rev. 31 (2014) 91–100, https://doi.org/10.1016/j.rser.2013.11.049.

[21] O.A. Alvarez-Silva, A.F. Osorio, C. Winter, Practical global salinity gradient energy potential, Renew. Sust. Energ. Rev. 60 (2016) 1387–1395, https://doi.org/10.1016/j.rser.2016.03.021.

[22] A.P. Straub, A. Deshmukh, M. Elimelech, Pressure-retarded osmosis for power generation from salinity gradients: is it viable? Energy Environ. Sci. 9 (2016) 31–48, https://doi.org/10.1039/c5ee02985f.

[23] N.Y. Yip, D. Brogioli, H.V.M. Hamelers, K. Nijmeijer, Salinity gradients for sustainable energy: primer, progress, and prospects, Environ. Sci. Technol. 50 (2016) 12072–12094, https://doi.org/10.1021/acs.est.6b03448.

[24] C. Seyfried, H. Palko, L. Dubbs, Potential local environmental impacts of salinity gradient energy: a review, Renew. Sust. Energ. Rev. 102 (2019) 111–120, https://doi.org/10.1016/j.rser.2018.12.003.

[25] R.R. Gonzales, A. Abdel-Wahab, S. Adham, D.S. Han, S. Phuntsho, W. Suwaileh, N. Hilal, H.K. Shon, Salinity gradient energy generation by pressure retarded osmosis: a review, Desalination 500 (2021) 114841, https://doi.org/10.1016/j.desal.2020.114841.

[26] S. Lin, Z. Wang, L. Wang, M. Elimelech, Salinity gradient energy is not a competitive source of renewable energy, Joule 8 (2024) 334–343, https://doi.org/10.1016/j.joule.2023.12.015.

[27] X. Tong, S. Liu, J. Crittenden, Y.S. Chen, Nanofluidic membranes to address the challenges of salinity gradient power harvesting, ACS Nano 15 (2021) 5838–5860, https://doi.org/10.1021/acsnano.0c09513.

[28] X.W. Han, W.B. Zhang, X.J. Ma, X. Zhou, Q. Zhang, X. Bao, Y.W. Guo, L. Zhang, J. P. Long, Review-technologies and materials for water salinity gradient energy harvesting, J. Electrochem. Soc. 168 (2021) 090505, https://doi.org/10.1149/1945-7111/ac201e.

[29] Z. Xie, Z. Xiang, X. Fu, Z. Lin, C. Jiao, K. Zheng, M. Yang, X. Qin, D. Ye, Decoupled ionic and electronic pathways for enhanced osmotic energy harvesting, ACS Energy Lett. 9 (2024) 2092–2100, https://doi.org/10.1021/acsenergylett.4c00320.

[30] D. Manikandan, S. Karishma, M. Kumar, P.K. Nayak, Salinity gradient induced blue energy generation using two-dimensional membranes, npj 2D Mater Appl. 8 (2024) 47, https://doi.org/10.1038/s41699-024-00486-5.

[31] J.D. Isaacs, R.J. Seymour, The ocean as a power resource, Int. J. Environ. Stud. 4 (1973) 201–205, https://doi.org/10.1080/00207237308709563.

[32] G.L. Wick, Power from salinity gradients, Energy 3 (1978) 95–100, https://doi.org/10.1016/0360-5442(78)90059-2.

[33] J.W. Post, J. Veerman, H.V.M. Hamelers, G.J.W. Euverink, S.J. Metz, K. Nymeijer, C.J.N. Buisman, Salinity-gradient power: evaluation of pressure-retarded osmosis and reverse electrodialysis, J. Membr. Sci. 288 (2007) 218–230, https://doi.org/10.1016/j.memsci.2006.11.018.

[34] R.J. Aaberg, Osmotic power, Refocus 4 (2003) 48–50, https://doi.org/10.1016/s1471-0846(04)00045-9.

[35] J. Kuleszo, C. Kroeze, J. Post, B.M. Fekete, The potential of blue energy for reducing emissions of CO_2 and non-CO_2 greenhouse gases, J. Integr. Environ. Sci. 7 (2010) 89–96, https://doi.org/10.1080/19438151003680850.

[36] L. Duan, R. Petroski, L. Wood, K. Caldeira, Stylized least-cost analysis of flexible nuclear power in deeply decarbonized electricity systems considering wind and solar resources worldwide, Nat. Energy 7 (2022) 260–269, https://doi.org/10.1038/s41560-022-00979-x.

[37] R.S. Norman, Water salination: a source of energy, Science 186 (1974) 350–352, https://doi.org/10.1126/science.186.4161.350.

[38] A.T. Jones, W. Finley, Recent development in salinity gradient power, in: Oceans 2003. Celebrating the Past... Teaming Toward the Future (IEEE Cat. No.03CH37492) 4, 2003, pp. 2284–2287, https://doi.org/10.1109/OCEANS.2003.178265.

[39] X. Gao, C. Kroeze, The effects of blue energy on future emissions of greenhouse gases and other atmospheric pollutants in China, J. Integr. Environ. Sci. 9 (2012) 177–190, https://doi.org/10.1080/1943815X.2012.701648.

[40] Y. Berrouche, P. Pillay, Determination of salinity gradient power potential in Québec, Canada, J. Renew. Sustain. Ener. 4 (2012) 053113, https://doi.org/10.1063/1.4754439.

[41] F. Helfer, C. Lemckert, Y.G. Anissimov, Osmotic power with pressure retarded osmosis: theory, performance and trends - a review, J. Membr. Sci. 453 (2014) 337–358, https://doi.org/10.1016/j.memsci.2013.10.053.

[42] F. Helfer, C. Lemckert, The power of salinity gradients: an Australian example, Renew. Sust. Energ. Rev. 50 (2015) 1–16, https://doi.org/10.1016/j.rser.2015.04.188.

[43] O. Alvarez-Silva, A.F. Osorio, Salinity gradient energy potential in Colombia considering site specific constraints, Renew. Energy 74 (2015) 737–748, https://doi.org/10.1016/j.renene.2014.08.074.

[44] M. Essalhi, A.H. Avci, F. Lipnizki, N. Tavajohi, The potential of salinity gradient energy based on natural and anthropogenic resources in Sweden, Renew. Energy 215 (2023) 118984, https://doi.org/10.1016/j.renene.2023.118984.

[45] S. Loeb, R.S. Norman, Osmotic power plants, Science 189 (1975) 654–655, https://doi.org/10.1126/science.189.4203.654.

[46] S. Loeb, Energy production at the Dead Sea by pressure-retarded osmosis: challenge or chimera? Desalination 120 (1998) 247–262, https://doi.org/10.1016/s0011-9164(98)00222-7.

[47] S. Loeb, One hundred and thirty benign and renewable megawatts from Great Salt Lake? The possibilities of hydroelectric power by pressure-retarded osmosis, Desalination 141 (2001) 85–91, https://doi.org/10.1016/S0011-9164(01)00392-7.

[48] S. Ortega, P. Stenzel, O. Alvarez-Silva, A.F. Osorio, Site-specific potential analysis for pressure retarded osmosis (PRO) power plants - the León River example, Renew. Energy 68 (2014) 466–474, https://doi.org/10.1016/j.renene.2014.02.033.

[49] A. Emdadi, P. Gikas, M. Farazaki, Y. Emami, Salinity gradient energy potential at the hyper saline Urmia Lake - Zarrinehrud River system in Iran, Renew. Energy 86 (2016) 154–162, https://doi.org/10.1016/j.renene.2015.08.015.

[50] S. Saki, N. Uzal, M. Gökçek, N. Ates, Predicting potential of pressure retarded osmosis power for different estuaries in Turkey, Environ. Prog. Sustain. Energy 38 (2019) 13085, https://doi.org/10.1002/ep.13085.

[51] S. Haddout, K.L. Priya, M. Rhazi, A. Jamali, M. Aghfir, A.M. Hoguane, I. Ljubenkov, Producing electricity at estuaries from salinity gradient: exergy analysis, Int. J. River Basin Manag. 20 (2020) 301–309, https://doi.org/10.1080/15715124.2020.1830784.

[52] K. Zachopoulos, N. Kokkos, C. Elmasides, G. Sylaios, Coupling hydrodynamic and energy production models for salinity gradient energy assessment in a salt-wedge estuary (Strymon River, Northern Greece), Energies 15 (2022) 2970, https://doi.org/10.3390/en15092970.

[53] A.F. Sitoe, A.M. Hoguane, S. Haddout, Salinity gradient energy potential of Mozambique estuaries, Mar. Georesour. Geotechnol. 42 (2023) 1–6, https://doi.org/10.1080/1064119x.2023.2248976.

[54] S. Haddout, K.L. Priya, Free energy production from salinity gradient power (SGP)-investigative results in two different estuaries, J. Eng. Thermophys. 32 (2023) 378–388, https://doi.org/10.1134/s1810232823020121.

[55] Ministry of Land, Infrastructure, Transport and Tourism: Status of Formulation of Basic River Maintenance Policy for First Class River Systems (accessed on 1 September 2024), https://www.mlit.go.jp/river/basic_info/jigyo_keikaku/gaiyou/seibi/.

[56] G.M. Barrow, Physical Chemistry, 6th edition, McGraw-Hill College, USA, 1996.

[57] P. Atkins, J. de Paula, J. Keeler, Atkins' Physical Chemistry, 12th edition, Oxford University Press, UK, 2022.

[58] G.Z. Ramon, B.J. Feinberg, E.M.V. Hoek, Membrane-based production of salinity-gradient power, Energy Environ. Sci. 4 (2011) 4423–4434, https://doi.org/10.1039/c1ee01913a.

[59] T. Thorsen, T. Holt, The potential for power production from salinity gradients by pressure retarded osmosis, J. Membr. Sci. 335 (2009) 103–110, https://doi.org/10.1016/j.memsci.2009.03.003.

[60] N.Y. Yip, M. Elimelech, Thermodynamic and energy efficiency analysis of power generation from natural salinity gradients by pressure retarded osmosis, Environ. Sci. Technol. 46 (2012) 5230–5239, https://doi.org/10.1021/es300060m.

[61] C. Forgacs, R.N. O'Brien, Utilization of membrane processes in the development of non-conventional renewable energy sources, Chem. Can. 31 (1979) 19–21.

[62] C. Forgacs, Recent developments in the utilization of salinity power, Desalination 40 (1982) 191–195, https://doi.org/10.1016/S0011-9164(00)88683-X.

[63] Geospatial Information Authority of Japan: The National Atlas of Japan (accessed on 1 September 2024), https://www.gsi.go.jp/atlas/atlas-e-etsuran.html.

[64] T. Ishikawa, R. Akoh, Application of running water-type retarding basin to old Kinu river floodplain, Japan, Hydrology 10 (2023) 94, https://doi.org/10.3390/hydrology10040094.

[65] Ministry of Land, Infrastructure, Transport and Tourism: Water Information Database (accessed on 1 September 2024) (in Japanese), http://www1.river.go.jp/index.html.

[66] R.E. Tharme, A global perspective on environmental flow assessment: emerging trends in the development and application of environmental flow methodologies for rivers, River Res. Appl. 19 (5–6) (2003) 397–441, https://doi.org/10.1002/rra.736.

[67] D.L. Tennant, Instream flow regimens for fish, wildlife, recreation and related environmental resources, Fisheries 1 (1976) 6–10, https://doi.org/10.1577/1548-8446(1976)001<0006:Ifrffw>2.0.Co;2.
[68] Website: Fukuoka District Waterworks Agency (in Japanese), https://www.f-suiki.or.jp/wp-content/uploads/2023/10/5683f686954e8bd95ac993ef013f1ccb.pdf.
[69] JST news (July 2013) p.12–13 (in Japanese), https://www.jst.go.jp/pr/jst-news/backnumber/2013/201307/pdf/2013_07_p12.pdf.
[70] Website: Goto City Renewable Energy Information (in Japanese), https://www.city.goto.nagasaki.jp/energy/030/030/20210616144118.html, June 2021.
[71] Website: Demonstration Test of Ocean Current Turbine System for Reliability and Economic Performance Evaluation. https://www.ihi.co.jp/en/technology/techinfo/contents_no/1200376_13586.html, 2023.
[72] Website: Power and Industry: The Kumejima Model's Potential to Revitalize Islands. https://www.jica.go.jp/english/information/topics/2023/20231117_01.html, 2023.
[73] N.Y. Yip, M. Elimelech, Comparison of energy efficiency and power density in pressure retarded osmosis and reverse electrodialysis, Environ. Sci. Technol. 48 (2014) 11002–11012, https://doi.org/10.1021/es5029316.
[74] M. Kurihara, M. Hanakawa, Mega-ton water system: Japanese national research and development project on seawater desalination and wastewater reclamation, Desalination 308 (2013) 131–137, https://doi.org/10.1016/j.desal.2012.07.038.
[75] A. Tanioka, Preface to the special issue on "pressure retarded osmosis in megaton water system project", Desalination 389 (2016) 15–17, https://doi.org/10.1016/j.desal.2016.02.013.
[76] M. Kurihara, H. Sakai, A. Tanioka, H. Tomioka, Role of pressure-retarded osmosis (PRO) in the mega-ton water project, Desalin. Water Treat. 57 (55) (2016) 26518–26528, https://doi.org/10.1080/19443994.2016.1168582.
[77] R. Makabe, T. Ueyama, H. Sakai, A. Tanioka, Commercial pressure retarded osmosis systems for seawater desalination plants, Membranes (Basel) 11 (2021) 33478037, https://doi.org/10.3390/membranes11010069.
[78] Y. Tanaka, M. Yasukawa, S. Goda, H. Sakurai, M. Shibuya, T. Takahashi, M. Kishimoto, M. Higa, H. Matsuyama, Experimental and simulation studies of two types of 5-inch scale hollow fiber membrane modules for pressure-retarded osmosis, Desalination 447 (2018) 133–146, https://doi.org/10.1016/j.desal.2018.09.015.
[79] T. Abo, S. Mehdizadeh, Y. Kakihana, M. Yasukawa, M. Higa, Power generation performance of a pilot-scale reverse electrodialysis (RED) stack, Bull. Soc. Sea Water Sci. Jpn. 73 (2019) 96–97, https://doi.org/10.11457/swsj.73.2_96.